

Incremental Static Analysis for the Seismic Performance Evaluation of a Peruvian R.C. Building

Ivan Mamani¹, Edson Quispe¹, Gram Rivas¹

¹Department of Civil Engineering, Universidad Peruana de Ciencias Aplicadas (UPC)

Av. La Marina 2810, San Miguel, Lima, Perú

u20201b843@upc.edu.pe; u20201c613@upc.edu.pe; pccigrri@upc.edu.pe

Abstract - In the present study, the incremental static or pushover analysis will be used, since it offers more accurate results compared to the linear analysis. Therefore, its application is indispensable for the evaluation of the seismic performance of a reinforced concrete structure composed of beams, columns and walls. This structure is a multi-family building of 6 levels, rectangular in shape with an area of 120 m². The methodology used allows obtaining the capacity of the structure against applied lateral loads, thus determining the performance levels for each level of seismic hazard according to the VISION 2000 guidelines. The study begins with an exhaustive analysis of the geometry, structural elements of the building, the use of standards and guidelines related to seismic resistance. However, two 3D structural models were created in Etabs V.21, called model 1 and model 2. In model 1, the non-linear model of plastic hinges for beams and columns will be taken into account, taking into consideration that the walls are hinged with fiber type hinges. On the other hand, for model 2, the nonlinear model of fiber-type hinges for columns, beams and walls will be taken into account. However, the indispensable resource is the ASCE 41-17/23 standard for the model with plastic hinges. On the other hand, we use the constitutive models of Mander and Park to define the behavior of concrete and steel in each fiber division. Then, the results of the capacity curve in each X and Y direction are compared. Finally, the pushover curve is sectorized to obtain the performance levels for frequent, occasional, rare and very rare earthquakes. Therefore, the findings in this article are useful for professionals engaged in structural engineering who are interested in the performance evaluation of a reinforced concrete structure or in other infrastructures that exist at the international level.

Keywords: Reinforced concrete structure (RC); performance evaluation; fiber hinge model, plastic hinge model; non-linear static analysis

1. Introduction

The seismic-resistant evaluation of buildings is one of the most complex challenges of structural engineering, especially in cities, which are extending their peripheral limits of urban development towards areas of high seismic hazard, generating more demanding requirements for the safety and durability of structures. To this end, multiple methodologies and modeling approaches have been proposed over the years to evaluate the capacity of buildings under seismic loads. However, linear static analysis is not adequate enough to understand the actual behavior of structural connections and materials when the elastic zone is exceeded. In addition, nonlinear analysis is usually not so much applied in standards due to its complexity, time and cost, as mentioned by [1]. Therefore, several researches propose methods that provide important data to evaluate the nonlinear behavior of a structure and procedures that help to properly understand the structural capacity.

This study aims to extend the understanding of building nonlinearity analysis to improve engineering robustness through a comparative analysis that evaluates the seismic behavior of a real building using different plasticity models: plastic hinges and fiber hinges. In such pushover analysis, incremental lateral forces are applied in any evaluated direction, but this method does not consider the dynamic implication [2]. On the other hand, it is important to note that in order to evaluate a structure by nonlinear procedures, it is crucial to have the guidelines of international standards such as ASCE 41-17, ATC-40 and VISION 2000. These standards are used to obtain the seismic behavior objectives. Similarly, the Etabs v.21 software is used as an invaluable tool for building analysis, providing reliable results.

Finally, this paper aims to provide an apt comparison of the actual behavior of a structure under any seismic loading, using plasticity models that are numerically grounded with seismic evaluation criteria [3] and optimized to provide a set of logical results that allow engineers to make reasonable decisions. Ultimately, we seek to compensate for the technical absence in the literature of nonlinear analysis.

2. Methods and Tools

2.1. Study Methodology

- Obtain structure data and define seismic performance targets according to [4] y [5]. for a multifamily building.
- We proceed to perform the 3D modeling in Etabs. V21, which are model 1 and model 2, on the building structure to be studied. Subsequently, the seismic parameters must be established according to [6].
- In addition, the hinges concentrated and distributed in each structural element of the building are assigned. In this case for model 1 and model 2, which will be simulated in the program mentioned above. Then the incremental lateral forces are applied in a triangular manner on each floor of the building.
- Obtain the pushover curve of the building and the seismic performance point, in the X direction and in the Y direction. For this purpose, the capacity spectrum method according to ATC-40 or FEMA 440 is used.
- Finally, perform the sectorization after bilinearizing the capacity curve. For this, the effective yield point must be taken into account. Also, obtain the structural capacity based on performance levels, which can be fully operational, operational, life safety, collapse prevention and collapse. Taking into account the level of seismic hazard, whether frequent, occasional, rare and very rare earthquakes.

2.2. Tools

The Etabs V.21 tool was important to perform the simulation of the building structure by applying the incremental forces in a nonlinear model. Where 3D structural models called model 1 (use of plastic and fiber hinges) and model 2 (use of fiber hinges) were made to obtain the seismic behavior of the studied building.

The Mander model for confined concrete “Fig. 1” will be used to evaluate the structural behavior. Likewise, for the stresses and deformations of reinforcing steel, the Park model “Fig. 2” will be taken into consideration.

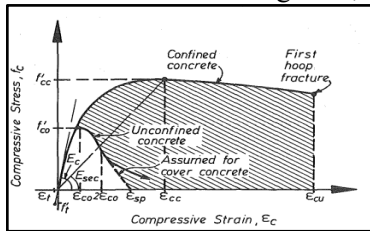


Fig. 1: Mander model for concrete.

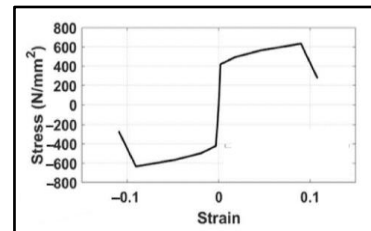


Fig. 2: Stress-strain for reinforcing steel.

In the “Fig. 3” shows the fiber assigned in each transverse selection of the column and beam, as well as the unconfined and confined concretes. On the other hand, the fiber type hinge in the reinforcing steel. This fiber is also assigned in structural wall elements.

In the “Fig. 4” shows how the plastic joint is only concentrated at the end, where the bending behavior is higher. In this case, the guidelines of [7] have been taken into account, from which the moments and rotational moments in each structural element are obtained.

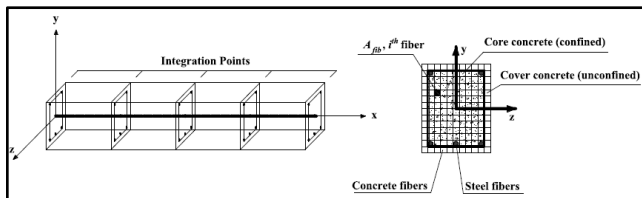


Fig. 3: Fiber hinge in the cross section of columns and beams.

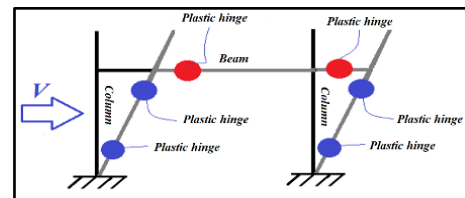


Fig. 4: Plastic hinge at each end of the structural element.

2.3. Description of the case study

The structure of the building under study is composed of reinforced concrete of structural elements only of columns, beams, slabs and shear walls, which can support the vertical and lateral loads. Likewise, it has 6 levels, the first level with a height of 3.2 m and the rest is 2.8 m. On the other hand, it has a floor plan with a total area of 120 m². In the X direction it is 6 m long and in the Y direction it is 20 m long.

Reinforced concrete with a compressive stress of $f'c = 210 \text{ kg/cm}^2$ is used. In addition, the weight is 2.4 tonf/m^3 and the Poisson's modulus is $2173706.51 \text{ tonf/m}^2$. On the other hand, grade 60 reinforcing steel will be used, where its yield strength is $fy = 4200 \text{ kgf/cm}^2$ and the elasticity model is $Es = 2 \times 10^7 \text{ tonf/m}^2$.

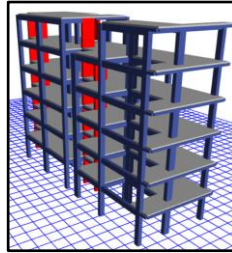


Fig. 5: The 3D model in Etabs V.21 of the building under study.

Also, lightened slabs and solid slabs are 0.20 m thick. On the other hand, there are two types of structural walls, which are: Wall 1 (SW-1) and wall 2 (SW-2) with thicknesses of 0.25 m and have a dimension of 1.05 m long. SW-1 is of type and therefore has an additional dimension of 0.40 m long. It is worth mentioning that SW-1 and SW-2 have 3/4" longitudinal reinforcements with 12 and 14 reinforcements, respectively. Moreover, the confinement reinforcement is 3/8" in both.

For a view of the structural elements, see Tables 1 y 2. They have written structural elements with different dimensions that are modeled in Etabs (3D), with their respective steels reinforcement longitudinal (RL) and confinement (RC).

Table 1: Structural elements of column.

Reinforced concrete	Symbology	Dimensions (m)	Steel Reinforcing	Take into account
Columns	C1	0.30 x 0.40	RL:8Ø5/8"; RC: Ø3/8"	Columns from floors 1st to floor 6th.
	C2	0.30 x 0.50		
	C3	L: 0.70 m; l: 0.30 m; a: 0.40 m	RL:14Ø5/8"; RC: Ø3/8"	
	C4	0.25 x 0.50	RL:8Ø5/8"; RC: Ø3/8"	
	C5	0.30 x 0.60	RL:10Ø5/8"; RC: Ø3/8"	
	C6	0.25 x 0.60	RL:8Ø5/8"; RC: Ø3/8"	
	C7	0.30 x 0.65	RL:12Ø5/8"; RC: Ø3/8"	

Table 2: Structural elements of the beam.

Reinforced concrete	Symbology	Dimensions (m)	Steel Reinforcing	Take into account
Cambered beams (CB)	B1	0.25 x 0.40 m	RL:6Ø5/8", 2Ø1/2"; RC: Ø3/8"	The beams from the 1st floor to the 6th floor.
	CB1;C	0.25 x 0.50 m	RL:8Ø5/8"; RC: Ø3/8"	
	CB2	0.25 x 0.50 m	RL:8Ø5/8"; RC: Ø3/8"	
	CB3	0.30 x 0.50 m	RL:8Ø5/8"; RC: Ø3/8"	
	CB4	0.30 x 0.50 m	RL:8Ø5/8"; RC: Ø3/8"	
	CB5	0.25 x 0.50 m	RL:10Ø5/8"; RC: Ø3/8"	
	CB6	0.25 x 0.50 m	RL:6Ø5/8"; RC: Ø3/8"	
	CB7	0.25 x 0.60 m	RL:8Ø5/8"; RC: Ø3/8"	
Flat beams (FB)	FB-1	0.30 x 0.20 m		From floor 1st to floor 6th.
	FB-2	0.40 x 0.20 m		
	FB-3	0.25 x 0.5 m		
	FB-4	0.25 x 0.5 m		

The considerations have been taken of different types of loads acting on the structure according to the E.030 standard. These are considered as permanent and non-permanent loads. The dead load or self-weight of structural elements is automatically calculated by the Etabs v.21 program. In addition, the dead load of partition walls, finishes and mezzanine brickwork is 100 kg/m^2 for each of them. On the other hand, the live load of the floor and roof is 200 kg/m^2 and 100 kg/m^2 , respectively.

The seismic parameters are determined in accordance with Peruvian standard E.030. Where the maximum ground acceleration is 0.45 g, the soil type is S1 (S=1), the seismic amplification factor is 2.5 seconds, the structure is type C (common use U=1) and with a damping fraction of 5%. From the above values, the pseudo-acceleration for each seismic hazard, whether design, frequent, occasional and very rare earthquakes, is obtained with equation 1 (see "Fig. 6").

$$S_a = (Z * U * C * S) / R * g \quad (1)$$

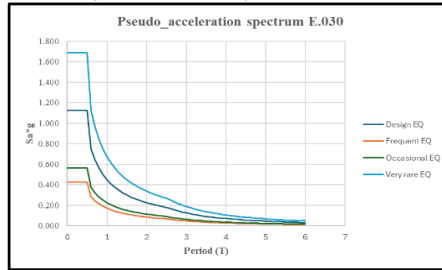


Fig. 6: Pseudo acceleration spectrum for each hazard level.

2.4. Sample assignment of plastic and fiber type hinges

In the “Fig. 7” shows the placement of the plastic hinges on column C1, taking into account the X and Y direction. In addition, in “Fig. 8” the fiber type hinge assigned in the cross section of the same structural element (C1) is taken into consideration, where the fiber areas representing for steel and reinforced concrete is equal to the gross area of the structural element (C1) modeled in Etabs V.21.

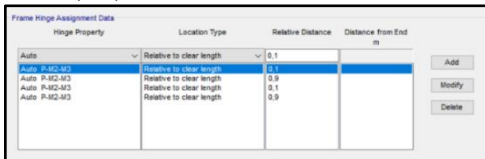


Fig. 7: Assignment of plastic hinges on a column.

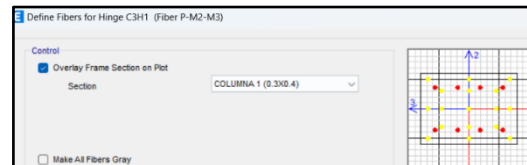


Fig. 8: Fiber type hinge assigned in a column.

3. Results

The results obtained after the development of the incremental analysis to know the nonlinear behavior of the structure are presented below. In the 3D modeling of the structure (model 1 and 2), the analysis was developed in the X and Y directions, using the plastic models. Fig. 9” shows the deformation progress of the plastic hinges, obtaining an ultimate deformation of 23 cm from a shear force of 190.2478 tonf (X axis) and 342.5371 tonf (Y axis). On the other hand, “Fig. 10” shows the formation of fiber type hinges, when the shear force is 243.29 tonf (X axis) and 419.29 tonf (Y axis) the ultimate deformation is 30 cm, in both cases.

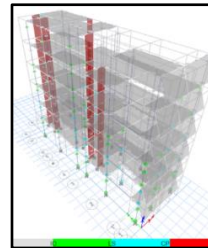
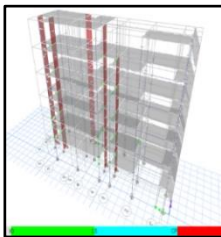


Fig. 9: Formation of plastic hinges on the model building. Fig. 10: Formation of fiber-type hinges in the modeled building.

We calculated the maximum elastic and inelastic drifts as a function of the deformations and the total height of the building (17.20 m) for both models. In addition, the specific performance requirements according to ATC-40 should be taken into account. Regarding this, [8] estimates that the appropriate level in seismic events is damage control, since it focuses on limiting the extent of deformations.

Table 3: Total drifts (plastic hinge and fiber hinge).

Drift	Model	Direction X	Direction Y	Drift	Model	Direction X	Direction Y
Drift Elastic	Model 1	0,002325581	0,001744186	Deriva Inelástico	Model 1	0,013372093	0,013368953
	Model 2	0,002172965	0,002342035		Model 2	0,01744186	0,01744186

3.1. Capacity curve of the structure using plastic and type fiber hinges

A capacity curve initiates an elastic behavior with a loss of stiffness until the inelastic behavior of the structure begins. This conception is exactly what is observed in “Fig. 11”, in model 1. Thus, a maximum displacement of 0.2289 m with a basal shear force of approximately 189.99 tonf was obtained in the X direction of the studied building. On the other hand, in the Y direction, a maximum displacement of 0.22889 m with a shear force of approximately 341.998 tonf was obtained (see “Fig. 11”). These numerical values are within the inelastic range in both directions of structural analysis.

In the same way, by using the fiber hinges (model 2) and its pushover application, the capacity curve in the X direction and in the Y direction was obtained. This graph shows the relationship of the basal shear force and the top displacement of the building to be studied, with a maximum displacement of 30 cm in both directions, shown in “Fig. 12”.

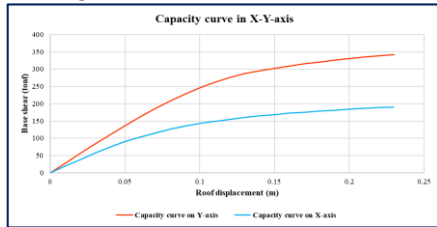


Fig. 11: Capacity curve in the X-Y direction (plastic hinge).

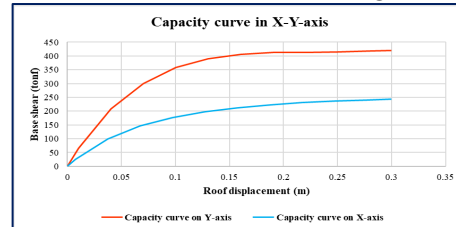


Fig. 12: Capacity curve in the X-Y direction (fiber hinge).

3.2. Seismic performance point in both directions with plastic hinge-model 1

Prior to obtaining the seismic performance points, the effective yield point in the X-Y direction must be obtained. This effective yield point is obtained after having bilinearized the capacity curve. Also, perform the sectorization for each seismic hazard in the X direction and in the Y direction, see “Fig. 13” and “Fig. 14”, respectively.

- The effective yield point in the X direction is: With lateral displacement (D_y) of 0.0749 m. And with a basal shear force (F_y) of 137.96 tonf.
- The effective yield point in the Y direction is: With lateral displacement (D_y) of 0.099 m. And with a basal shear force (F_y) of 266.86 tonf.

Below, in the table 4 shows the seismic performance point, having the values of the basal shear forces and their displacement, for each seismic hazard.

Table 4: Seismic performance point-Plastic hinges.

Direction	Seismic hazard	Basal Shear (V) (tonf)	Displacement (m)	Direction	Seismic hazard	Basal Shear (V) (tonf)	Displacement (m)
X-axis	Frequent EQ	86.18	0.047	Y-axis	Frequent EQ	108.79	0.039
	Occasional EQ	106.16	0.062		Occasional EQ	144.96	0.053
	Rare EQ	161.23	0.132		Rare EQ	258.36	0.108
	Very Rare EQ	189.39	0.225		Very Rare EQ	301.71	0.149

These points obtained are important to obtain the level of seismic performance, which can be operational, functional, life safety, collapse prevention and collapse. See “Fig. 13” and “Fig. 14” for the points assigned for each seismic hazard.

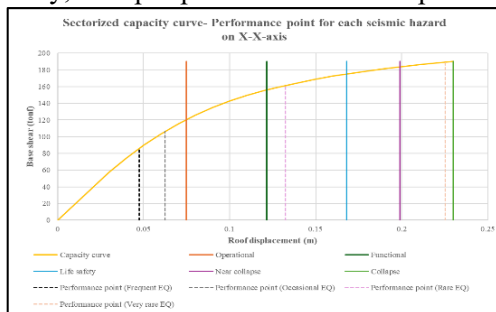


Fig. 13: Sectorized curve and placement of performance points on X-axis (plastic hinge).

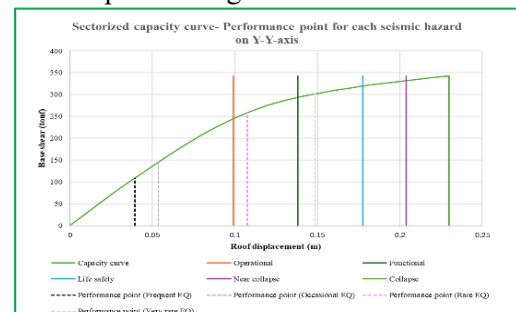


Fig. 14: Sectorized curve and placement of performance points on Y-axis (plastic hinge).

3.3. Seismic performance point in both directions with fiber hinge-model 2.

Similar to the modeling of plastic hinges in this fiber section, the effective yield point in the X-Y direction must be achieved. On the one hand, develop the bilinearization and sectorization of the capacity curve achieved from the use of fiber hinges, for this, observe “Fig. 15” and “Fig. 16”, which is sectorized the capacity curve taking into account the effective yield points shown below:

- The effective yield point in the X direction is: With lateral displacement (D_y) of 0.074138 m. And with a basal shear force (F_y) of 185.3321 tonf.
- The effective yield point in the Y direction is: With lateral displacement (D_y) of 0.074213 m. And with a basal shear force (F_y) of 371.3447 tonf.

In the table 5 shows the seismic performance points in the X and Y directions.

Table 5: Seismic performance point-Fiber hinges.

Direction	Seismic hazard	Basal Shear (V) (tonf)	Displacement (m)	Direction	Seismic hazard	Basal Shear (V) (tonf)	Displacement (m)
X-axis	Frequent EQ	135.63	0.0603	Y-axis	Frequent EQ	223.75	0.0452
	Occasional EQ	154.82	0.0754		Occasional EQ	255.32	0.0555
	Rare EQ	194.79	0.123		Rare EQ	352.48	0.0973
	Very Rare EQ	219.52	0.179		Very Rare EQ	392.28	0.134

From the achieved performance points, the sectorized pushover curve is placed in order to know the seismic performance level of the studied structure, which is made of reinforced concrete, as shown in Figures 15 and 16, for the X direction and Y direction, respectively.

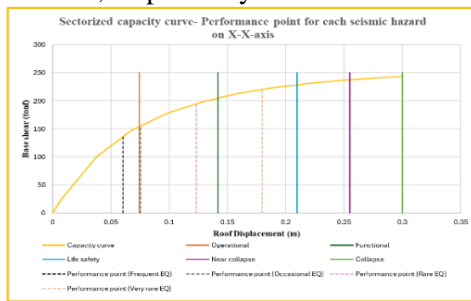


Fig. 15: Sectorized curve and performance points on X-axis (fiber hinge).

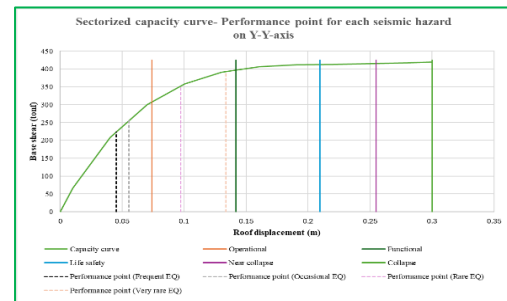


Fig. 16: Sectorized curve and performance points on Y-axis (fiber hinge).

3.4. Obtaining performance levels in the X-Y direction when using plastic hinges - model 1

The performance level for each seismic hazard is obtained according to VISION 2000. The levels obtained in the X-Y direction are described below.

- According to “Fig. 13” the performance level for the frequent and occasional earthquake is operational in the X direction. For the rare and very rare earthquake the performance level is life safety and collapse respectively.
- According to “Fig. 14” in the Y direction, the seismic performance level for the frequent and occasional earthquake is operational. Likewise, for the rare earthquake the level is functional. Finally, for the very rare earthquake it is life safety.

3.5. Obtaining performance levels in the X-Y direction when using fiber hinges-model 2

For the fiber modeling, the SEAOC (1995) guide is used in the same way, in order to obtain the performance levels for each earthquake. The levels obtained in the X-Y direction are described below.

- According to “Fig. 15” the performance level for the frequent earthquake is operational. It is functional for the occasional earthquake in the X direction. For the rare and very rare earthquake the performance level is functional and life safety, respectively.
- According to “Fig. 16” in the Y direction, the seismic performance level for the frequent and occasional earthquake is operational. Finally, for the rare and very rare earthquake the performance level is functional.

4. Analysis and Interpretation

The capacity curves obtained from the nonlinear models called: model 1 and model 2, are estimated to have similar behavior in the X direction, although the shear stresses obtained with model 2 tend to be higher (see “Fig. 17”).

After performing the pushover analysis in both nonlinear models for the X direction, we reached a numerical consensus, in which a better shear capture is expected where there is a larger stress distribution (model 2). On the other hand, the global moment-rotation system of model 1 describes its capacity limit due to the increasing phases of bending moment in the vulnerable zones of the element, resulting in a simplified realistic analysis [9].

The shear forces vary significantly (see “Fig. 18”). The ultimate state of model 2 is generated when it reaches a displacement of 30 cm, the effect of a shear force of 419.29 ton-f. In contrast, in model 1, a displacement of 29 cm induced by a shear of 246.4593 ton-f was reached.

Particularly in the Y direction, it is understood that fiber hinges present higher thrust forces, this effect occurs because the internal momentum of the structure changes when it reaches the elastic limit. That is, the plasticized fiber yields the bending moment to the non-plasticized fiber, thus deserving a higher thrust force. On the contrary, plastic joints do not undergo plasticization distributed throughout the section, so that the thrust forces are regular up to the ultimate state.

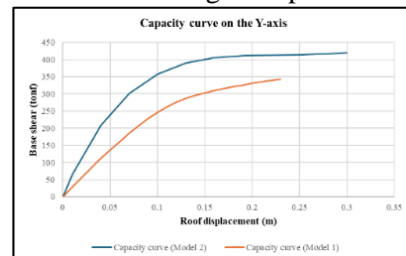
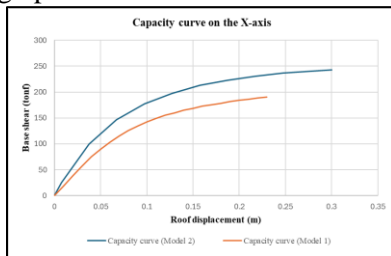


Fig. 17: Capacity curve of plastic and fiber hinges on the X-axis.

Fig. 18: Capacity curve of plastic and fiber hinges on the Y-axis.

However, the detailed comparative analyses of the performance levels are presented (see Table 6). In terms of structural resistance progression, it means that the absorption capacity and damage distribution of the model 1 in the X direction are low, since it notoriously generates more critical performance points. In contrast, the model 2 avoids overloading critical areas. That is, instead of allowing the structural elements to absorb all the energy until they reach their yield point, it distributes the loads evenly. This result is confirmed by scientific research such as that of [10].

Table 6: Performance levels of plastic hinges and fiber hinges on X-axis.

Seismic Hazard	Building performance level - SEAOC			
	Fully operational	Operational	Life safety	Collapse prevention
Frequent EQ (43 years)	Model 2	Model 1		
Occasional EQ (72 years)		Model 2		
Rare EQ (475 years)		Model 2		Model 1
Very rare EQ (970 years)			Model 2	

In the Y direction (see Table 7), it is observed that model 2 still reflects better the distribution of forces, estimating better the ductility and displacements, since it attributes the properties of concrete, steel and degradation for each fiber of the cross-section of the structural element. In addition, in model 1, reduction factors are assigned to the effective stiffness for better performance, as indicated by ASCE 41-17. This last analysis validates the loss of stability of the building for high seismic demands of model 1 and model 2, reaching the agreement that the plastic hinges have a greater degradation of stiffness.

Table 7: Performance levels of plastic hinges and fiber hinges on Y-axis.

Seismic Risk	Building performance level - SEAOC			
	Fully operational	Operational	Life safety	Collapse prevention
Frequent EQ (43 years)	Model 2	Model 1		
Occasional EQ (72 years)	Model 2	Model 1		
Rare EQ (475 years)		Model 2	Model 1	
Very rare EQ (970 years)		Model 2		Model 1

5. Conclusions

A comparative analysis of two nonlinear modeling approaches has been carried out to examine the seismic behavior of a reinforced concrete multifamily building, model 1 meets the current requirements of ASCE 41-17 and ACI 318-19 codes, model 2 is numerically adapted with academic grade research standardized with scientific methodologies. From this, the capacity curves were obtained and sectorized to classify the performance points achieved in terms of demand and capacity using the SEAOC VISION 2000 model.

It was argued that the behavior of the building is not adequate enough to resist high seismic demands in the X direction, due to the distribution of walls concentrated in one zone, generating excessive torsion and impairing its seismic response. On the other hand, it was also verified that, both in the X and Y directions, model 2 resorts to the increase of the shear force in the transition of a fiber layer in its creep limit with a fiber in the elastic zone. In contrast, model 1 generates force increases without significant alterations due to simplified plasticization at the ends.

The percentage difference of the inelastic drifts in model 2 is 23.35% higher than in model 1 in the X and Y directions, which means that the structure with model 2 is more flexible and ductile. This difference occurs due to the correct load transition in the structural element section, which is more realistic to represent the deformations compared to model 1.

The force distribution capability with model 2 is better for performing a nonlinear static analysis, since its configuration redistributes the loads applied to the structural elements. On the other hand, model 1 generates deformations in areas of maximum moments, the stress distribution is not evaluated in detail. However, it better represents the stiffness degradation due to concrete cracking. That is, the capacity of the building is significantly reduced after exceeding the yield strength. This approach is supported by ASCE 41-17 to provide numerical methods based on experimental tests to represent a more realistic behavior for the stiffness decrease effect in the creep zone.

Acknowledgements

A la Dirección de Investigación de la Universidad Peruana de Ciencias Aplicadas por el apoyo brindado para realización de este trabajo de investigación a través del incentivo UPC-EXPOST-2025-1. Financial support: Universidad Peruana de Ciencias Aplicadas / UPC-EXPOST-2025-1.

References

- [1] S F. A. Çağlar and T. Tatar, “Fiber-based modeling strategies of RC columns,” *Acad. Platform J. Nat. Hazards Disaster Manag.*, vol. 2, no. 2, pp. 85–95, Dec. 2021.
- [2] R. Suwondo and M. B. U. Arief, “Evaluating the seismic performance of low-rise concrete buildings using nonlinear static analysis,” *Civil Engineering and Architecture*, vol. 11, no. 4, pp. 1976–1983, Feb. 2023.
- [3] A. Abd-Elhamed, S. Mahmoud, and K. S. Alotaibi, “Nonlinear analysis of reinforced concrete buildings with different heights and floor systems,” *Scientific Reports*, vol. 13, no. 1, 2023.
- [4] Structural Engineers Association of California, *Performance-Based Seismic Engineering of Buildings, SEAOC-Vision 2000*, SEAOC, Oakland, CA, Oct. 1995.
- [5] Applied Technology Council, *Seismic evaluation and retrofit of concrete buildings, ATC-40*, vol. 1–2, Redwood City, CA: ATC, 1996.
- [6] Ministry of Housing, Construction and Sanitation, *Technical Standard E.030: Seismic Design, in Peruvian Technical Standard*, NTP E030 1997-2018, Lima, PE, 2018.
- [7] American Society of Civil Engineers, *Seismic Evaluation and Retrofit of Existing Buildings, ASCE/SEI 41*. Reston, VA: ASCE, Apr. 2017.
- [8] Masrilayante, Y. A. Hasibuan, R. Kurniawan, J. Sunaryati, and R. Aidil Fitrah, “Performance evaluation of high-rise apartment building using pushover analysis,” in *Proceedings of the E3S Web of Conferences*, 2023, vol. 429, p. 05024.
- [9] N. Pereira, D. Skoulidou, and X. Romão, “Closed-form expressions for partial safety factors used in the seismic assessment of existing RC buildings,” *Bulletin of Earthquake Engineering*, vol. 22, no. 3, pp. 997–1032, Nov. 2023.
- [10] F. Barbagallo, M. Bosco, A. Floridia, E. M. Marino, D. Panarelli, P. P. Rossi, and N. Spinella, “Calibration of the length of the plastic hinge for numerical models of reinforced concrete members,” *Buildings*, vol. 12, no. 10, p. 1603, Oct. 2022.